Quantitative Bremsstrahlung SPECT Imaging: Attenuation-Corrected Activity Determination

Jeffry A. Siegel

Department of Radiation Oncology, Cooper Hospital/University Medical Center, Camden, New Jersey

Bremsstrahlung SPECT imaging and activity quantitation have been performed using ^{32}P-chromic phosphate. **Methods:** Attenuation correction was applied to the reconstructed transverse SPECT slices using a commercially available first-order postprocessing algorithm. The patient's body contour was defined through the use of four externally placed sources and attenuation correction was then performed with an experimentally determined effective linear attenuation coefficient for ^{32}P. Phantom studies were performed to determine the activity needed in the four external sources and also to validate absolute activity analysis on the reconstructed SPECT slices. A computer algorithm was written to facilitate ROI activity determination based on a fixed threshold method. Four cancer patients enrolled in clinical Phase I protocols were injected with 2.5 million particles of macroaggregated albumin followed by colloidal ^{32}P-chromic phosphate by direct interstitial injection into the tumor-bearing region under CT guidance. The in vivo ^{32}P activity distribution was restricted to a small volume with minimal background activity. SPECT images were obtained in these patients and the activity of ^{32}P present in the tumors was calculated from their attenuation-corrected reconstructed SPECT slices. **Results:** The effective linear attenuation coefficient for ^{32}P was determined to be 0.13 cm^{-1}. A fixed 39% threshold was best for activity calculation since it provided the best correlation between known and measured activity levels in the phantom. The calculated activities were within 16.9% of the actual activities in the patients studied. **Conclusion:** Accurate quantitative bremsstrahlung SPECT imaging with a commercially available postprocessing attenuation correction algorithm can be performed in a clinical setting.

Key Words: bremsstrahlung; quantitative SPECT imaging; phosphorus-32; attenuation correction; radionuclide therapy

J Nucl Med 1994; 35:1213–1216

The ability to perform quantitative SPECT is affected by a number of parameters, including attenuation and scatter corrections, limited spatial and energy resolution, septal penetration by high-energy photons and statistical noise due to low count densities. The work reported here investigates an established postprocessing method of attenuation correction for bremsstrahlung SPECT using ^{32}P-chromic phosphate. The attenuation compensation technique allows the determination of volume of distribution and absolute activity of the beta-emitting radionuclide.

The attenuation correction algorithms used in SPECT can be classified into three categories: preprocessing correction, intrinsic correction and postprocessing correction (*1*). The most widely used approach in current commercial SPECT systems is the postprocessing algorithm (*2*), wherein the image is first reconstructed using filtered backprojection and then multiplied on a voxel-by-voxel basis by a mean depth-dependent attenuation correction.

Any attenuation correction algorithm in SPECT first requires the accurate delineation of the body contour (*1*). The measurement of the body contour has been performed using the object emission data, either from the photopeak (*3,4*), a Compton scatter window (*5*) or by other acquisition protocols including the use of point sources (*6*), a ring source (*1*), a 90° Compton scatter source (*7*) or a transmission SPECT study (*8,9*). The body is then fit to either an elliptical, convex or arbitrary boundary (*1*). Except for the transmission study, all attenuation methods based on this boundary information assume that the patient is uniform within the boundary.

We have previously described bremsstrahlung SPECT scintigraphy in a group of research subjects who were participants in Phase I therapeutic trials utilizing 2.5 million particles of macroaggregated albumin followed by colloidal ^{32}P-chromic phosphate (*10*). The albumin and ^{32}P were administered by direct interstitial injection into the tumor-bearing region under CT guidance. In the vast majority of cases, the ^{32}P remained in a well-defined area in the tumor with little observed migration out of the injection site. Attenuation correction was not applied in these studies.

The objective of the present study was to determine the accuracy of activity quantitation for bremsstrahlung SPECT studies using Chang's postprocessing method (*11*) of attenuation compensation with a computer-generated body contour based on four externally placed sources and

Received Oct. 18, 1993; revision accepted Mar. 23, 1994.

For correspondence or reprints contact: Jeffry A. Siegel, PhD, Dept. of Radiation Oncology, Cooper Hospital/University Medical Center, One Cooper Plaza, Camden, NJ 08103.

an experimentally measured effective linear attenuation coefficient for ^{32}P.

MATERIALS AND METHODS

Determination of Effective Linear Attenuation Coefficient

A Siemens Multispect 2 Gamma Camera System (Siemens Gammasonics, Hoffman Estates, IL) fitted with medium-energy parallel-hole collimators and interfaced to an ICON computer was employed for these studies. An energy window setting of 100 keV ± 25% was used, since we have previously shown that this narrow window setting has optimal resolution characteristics for ^{32}P (*10*). A point source containing 196 MBq of ^{32}P-chromic phosphate was prepared and bremsstrahlung images were acquired in the planar mode for 5 min at various depths in tissue-equivalent material (4.03 cm, 9.53 cm and 15.47 cm) and in air at these same distances. Regions of interest (ROIs) were drawn to obtain the source counts at all investigated depths for the transmission factor determination. The transmission factor data were analyzed by an exponential least-squares fitting routine to determine the effective linear attenuation coefficient for ^{32}P.

SPECT Technique

SPECT imaging was performed using the same dual-headed gamma camera system as described above. Energy window settings of 100 keV ± 25% and medium-energy parallel-hole collimators were used for each head (*10*). Four distributed sources of ^{32}P (2-cc vials, 2.5 cm length) containing approximately 3.7 MBq each were first placed directly on the patient in the anterior, posterior, right lateral and left lateral positions. Data were then acquired with 32 projections over 180° for each camera head (for a total of 64 projections over 360°) for 20 sec using the auto contour rotation mode into a 64 × 64-image matrix. A single projection image in the patient and phantom studies typically contained 15K–20K counts. The raw data were reconstructed by filtered backprojection using a fifth order Butterworth window with a cutoff at 0.6 of the Nyquist frequency (0.31 cycles/cm) in the transaxial, sagittal and coronal planes. The reconstructed slices were one pixel thick (9.6 mm). The patient's body contour was then determined on the reconstructed transverse slices using the Auto Boundary method option on the ICON computer or a manually drawn ellipse by ensuring that the boundary intersected all four of the externally placed sources. Chang's method (*11*) of attenuation correction was applied to the transverse reconstructed slices using the body contour for each transverse slice and the experimentally determined effective linear attenuation coefficient.

Quantitative analysis was then applied to the various activity distributions seen on the attenuation-corrected transaxial, sagittal or coronal slices based on a fixed threshold method (*10*). A computer algorithm was written in PASCAL to calculate ROI volumes and activities. All reconstructed slices (transaxial, coronal or sagittal) spanning the object are first added together to form a sum image. The operator is then prompted to draw a ROI around the object. This boundary defines a mask to be applied to each included slice. The program then searches through all the selected slices to find the five hottest voxels which are then averaged to represent the maximum voxel count. The operator is then prompted to select a threshold value, i.e., a percentage of the maximum voxel count in the masked region. Only voxels containing counts greater than this threshold value will be subsequently included in the activity calculation. This threshold value was determined from phantom studies. At this point, the program again searches through all the selected slices, this time only including voxels with counts greater than the threshold value. The activity (MBq) is then determined from the sum of the counts in the included voxels divided by the acquisition time and an independently acquired counting rate per unit activity system calibration factor (cps/MBq).

Phantom Studies

To determine the optimum threshold value to be used in the algorithm for activity determination, a hollow, 5-cm diameter sphere (volume = 65 cc) was filled with 21.7 MBq of ^{32}P-chromic phosphate. The source was then placed in a water-filled organ-scanning phantom (The Phantom Laboratory, Salem, NY) and four sources of ^{32}P were placed on the phantom in the anterior, posterior, right lateral and left lateral positions. The externally placed sources contained 0.56 MBq, 1.11 MBq, 1.85 MBq and 3.7 MBq of ^{32}P-chromic phosphate. A SPECT study was performed to determine the activity required for visualization of the external sources on the transverse reconstructed SPECT slices using the clinical acquisition parameters described above. Once determined, the other three sources were filled with this activity level, and a second SPECT study was performed and the activity in the sphere was determined from the attenuation-corrected reconstructed SPECT slices. The sphere was then filled with 308 MBq of ^{32}P-chromic phosphate and another SPECT study and activity determination was performed.

Patient Studies

Clinical Phase I studies have been carried out in nonresectable pancreatic cancer, nonresectable nonoat cell lung cancer, advanced head and neck cancer and liver metastases (*10*). The Phase I trial is based on the direct interstitial administration of 2.5 million particles of macroaggregated albumin followed by colloidal ^{32}P-chromic phosphate into the tumor-bearing region performed under CT guidance. All patients signed an informed consent form approved by our Institutional Review Committee. Four patients were studied for this preliminary investigation. Patient 1 was injected with 217 MBq of ^{32}P-chromic phosphate into a liver tumor. Patient 2 was injected with 110 MBq of ^{32}P-chromic phosphate into a pancreatic tumor. Patient 3 was injected with 681 MBq of ^{32}P-chromic phosphate into a lung tumor. Patient 4 was injected with 668 MBq of the same material into a pancreatic tumor. The patients were imaged using the same equipment and techniques as described above. SPECT imaging was performed on Day 3 for the first two patients, on Day 13 for the third patient, and on Day 4 for the fourth patient. Attenuation correction and activity determination were performed on the ^{32}P-reconstructed SPECT slices using the methods described above.

RESULTS

The effective linear attenuation coefficient for ^{32}P was determined to be 0.13 cm^{-1}, with a correlation coefficient of −0.999, from analysis of the transmission factor versus depth experimental data.

The activity required for visualization of the four externally placed sources was determined to be 3.7 MBq. The reconstructed transverse slices for the phantom study are shown in Figure 1. The four external sources are clearly seen surrounding the ^{32}P-filled sphere. Also shown is the computer-generated contour of the organ-scanning phantom in one of the reconstructed slices. The phantom study

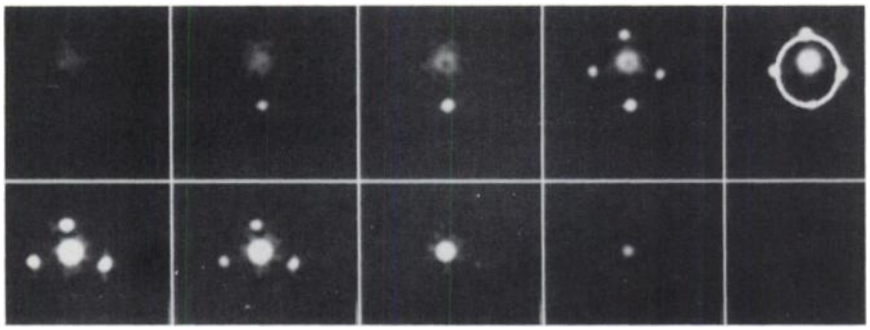

FIGURE 1. Reconstructed one-pixel thick (9.6 mm) transverse sections of phantom (^{32}P-filled 65-cc sphere) with contour shown on one slice.

indicated that a 39% threshold was optimal for activity determination on the attenuation-corrected reconstructed SPECT slices since it provided the best correlation between known and measured activity levels in the sphere. The 21.7-MBq activity measured 19.9 MBq (−8.2%) and the 308-MBq activity measured 329 MBq (+6.8%).

Figure 2 shows the reconstructed transverse SPECT slices for Patient 3. The bremsstrahlung images in the four patients studied indicated that there was no leakage of ^{32}P out of the injection site. The activity present in the lesion at the time of the SPECT imaging study was therefore calculated by physical decay using the physical half-life of ^{32}P. The results of the activity determination in the four patients studied were: Patient 1, calculated 175 MBq activity measured 155 MBq (−11.5%); Patient 2, calculated 92.7 MBq activity measured 96.5 MBq (+4.0%); Patient 3, calculated 353 MBq activity measured 318 MBq (−10.0%); and Patient 4, calculated 550 MBq activity measured 458 MBq (−16.9%).

DISCUSSION

Reasonably accurate and precise quantitative SPECT imaging is clinically feasible, even without sophisticated scatter corrections, at least in uniformly attenuating parts of the body such as the abdomen and pelvis (*2*). Using a postprocessing algorithm, the most commonly used approach in commercial SPECT systems, several investigators have obtained fairly accurate activity estimates (*2,12,13*). Osborne et al. (*13*) obtained good activity agreement even in a canine thorax despite the fact that the thorax attenuates nonuniformly.

SPECT bremsstrahlung imaging has been reported by a number of investigators using ^{32}P (*10,14,15*) and ^{90}Y (*16*). In the present study, a first-order postprocessing attenuation correction using Chang's method (*11*) was applied to reconstructed transverse ^{32}P bremsstrahlung SPECT slices using a computer-generated body contour and an effective linear attenuation coefficient of 0.13 cm^{-1}. The body contour was determined in the reconstructed transverse slices using four externally placed sources and a commercially supplied computer algorithm. Distributed sources were used in order to avoid the necessity of the rigorous coplanar placement required for point sources. These ancillary sources were necessary since the body outline could not be obtained from the emission data itself in our case. The 3.7-MBq activity in these sources was sufficient for their visualization and therefore, body contour delineation in all the patients studied. The measured attenuation coefficient was in good agreement with that reported by Clarke et al. (*17*) and the high degree of correlation in its measured data suggests that attenuation corrections can be applied using the Chang algorithm for SPECT imaging.

The agreement of the phantom and patient activities as measured by SPECT compared to the actual activities was excellent. The phantom studies performed represented clinically relevant conditions, i.e., isolated sources with little or no background activity, as would be anticipated for our direct interstitial administration technique. For other routes of radionuclide administration, there are often multiple source regions with associated background activities, which limits image contrast and contributes scatter to the total counts in the various source ROIs. In situations where the activity is more widely distributed, e.g., antibody imaging using ^{90}Y for radioimmunotherapy, it may be necessary to apply a resolution recovery filter (*17–20*) to minimize cross talk due to photon scattering between adjacent

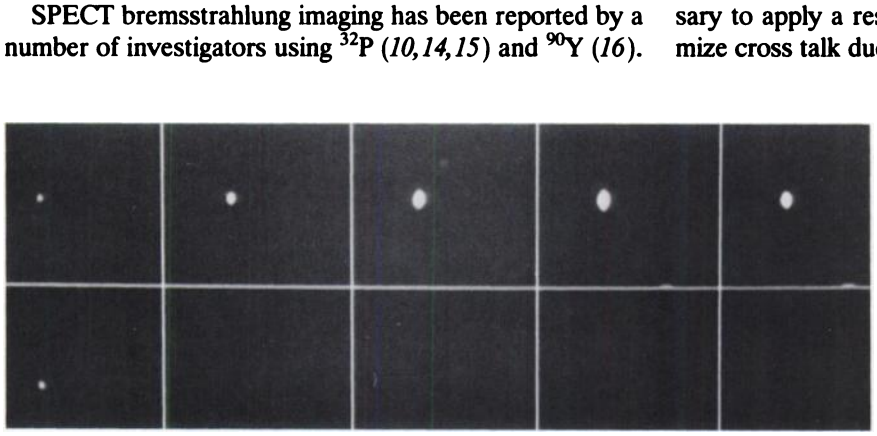

FIGURE 2. Reconstructed one-pixel thick (9.6 mm) transverse sections of Patient 3 injected with ^{32}P-chromic phosphate directly into a 33-cc lung tumor.

sources. The 39% threshold used for activity quantitation was identical to our previously reported value for volume determination (*10*).

We conclude that reasonably accurate quantitative bremsstrahlung SPECT imaging, for limited source region distribution with minimal background activity, can be performed in a clinical setting with a commercially available first-order postprocessing attenuation correction algorithm.

REFERENCES

1. Gullberg GT, Malko JA, Eisner RL. Boundary detection methods for attenuation correction in single photon emission computed tomography. In: Esser P, ed. *Emission computed tomography: current trends*. New York: The Society of Nuclear Medicine; 1983:33–53.
2. Zanzonico PB, Bigler RE, Sgouros G, Strauss A. Quantitative SPECT in radiation dosimetry. *Semin Nucl Med* 1978;19:47–61.
3. Webb S, Flower MA, Ott RJ, Leach MO. A comparison of attenuation correction methods for quantitative single photon emission computed tomography. *Phys Med Biol* 1983;28:1045–1056.
4. Hosoba M, Wani H, Toyama H, Murata H, Tanaka E. Automated body contour detection in SPECT: effects on quantitative studies. *J Nucl Med* 1986;27:1184–1191.
5. Jaszczak RJ, Chang LT, Stein NA, Moore FE. Whole body single-photon emission computed tomography using large field of view scintillation cameras. *Phys Med Biol* 1979;24:1123–1143.
6. Larsson SA. Gamma camera emission tomography. *Acta Radiologica Suppl* 1980;363:1–75.
7. Macey DJ, DeNardo GL, DeNardo SJ. Comparison of three boundary detection methods for SPECT using compton scattered photons. *J Nucl Med* 1988;29:203–207.
8. Maeda H, Ito H, Ishii Y, et al. Determination of the pleural edge by gamma ray transmission computed tomography. *J Nucl Med* 1981;22:815–817.
9. Malko JA, Gullberg GT, Kowalsky WP, Van Heertum RL. A count-based algorithm for attenuation-corrected volume determination using data from an external flood source. *J Nucl Med* 1985;26:194–200.
10. Siegel JA, Whyte-Ellis S, Zeiger LS, Order SE, Wallner PE. Bremsstrahlung SPECT imaging and volume quantitation with phosphorus-32. *Antibody Immunoconj Radiopharm* 1994;7:1–10.
11. Chang LT. A method for attenuation correction in radionuclide computed tomography. *IEEE Trans Nucl Sci* 1978;NS-25:638–642.
12. Jaszczak RJ, Coleman RE, Whitehead FR. Physical factors affecting quantitative measurements using camera-based single photon emission computed tomography (SPECT). *IEEE Trans Nucl Sci* 1981;NS-28:69–80.
13. Osborne D, Jaszczak RJ, Coleman RE, Greer K, Lischko M. In vivo regional quantitation of intrathoracic ^{99m}Tc using SPECT: concise communication. *J Nucl Med* 1982;23:446–450.
14. Ott RJ, Flower MA, Jones A, McCready VR. The measurement of radiation doses from ^{32}P-chromic phosphate therapy of the peritoneum using SPECT. *Eur J Nucl Med* 1985;11:305–308.
15. Cullom SJ, Clarke LP, Madden JA, King MA. Resolution and contrast recovery from bremsstrahlung images using the count dependent Metz filter. In: King MA, Zimmerman RE, Links JM, eds. *Imaging hardware and software for nuclear medicine*. New York: American Institute of Physics, Inc.; 1988:212–215.
16. Smith T, Crawley JCW, Shawe DJ, Gumpel JM. SPECT using bremsstrahlung to quantify ^{90}Y uptake in Baker's cysts: its application in radiation synovectomy of the knee. *Eur J Nucl Med* 1988;14:498–503.
17. Clarke LP, Cullom SJ, Shaw R, et al. Bremsstrahlung imaging using the gamma camera: factors affecting attenuation. *J Nucl Med* 1992;33:161–166.
18. King MA, Coleman M, Penney BC, Glick SJ. Activity quantitation in SPECT: a study of prereconstruction Metz filtering and use of the scatter degradation factor. *Med Phys* 1991;18:184–189.
19. Penney BC, King MA, Schwinger RB, Baker SP, Doherty PW. Modifying constrained least-squares restoration for application to single-photon emission tomography projection images. *Med Phys* 1988;15:334–342.
20. Qian W, Kallergi M, Clarke LP. Order statistic-neural network hybrid filters for gamma camera bremsstrahlung image restoration. *IEEE Trans Med Imaging* 1993;12:58–64.